JOURNAL OF CHEMOMETRICS, VOL. 10, 615–630 (1996)

SPECTRAL RESOLUTION AND PREDICTION OF SLIT WIDTHS IN FLUORESCENCE SPECTROSCOPY BY TWO- AND THREE-WAY METHODS

LARS NØRGAARD

Food Technology, Royal Veterinary and Agricultural University, Department of Dairy and Food Science, Thorvaldsensvej 40, DK-1871 Frederiksberg C, Denmark

SUMMARY

Modern spectrofluorometers have several instrumental settings to be adjusted and decided on before sample measurement, e.g. excitation and emission slit widths, emission scan velocity and spectral ranges to be recorded. The influences of these settings on the recorded spectra are crucial, particularly when applying full fluorescence spectra in the analysis of a given problem. The effect on the fluorescence emission spectra when changing the slit widths is studied in detail by recording the emission spectra of an ovalene standard block at all possible excitation (3–15 nm) and emission (3–20 nm) slit width combinations. By the two-way curve resolution method alternating regression (AR) it is possible to resolve the emission spectra into three hidden spectra describing the coarse, medium coarse/fine and fine structure of the recorded spectra. By the three-way methods PARAFAC and Tucker it is possible to separate the effects of both the excitation and emission slit widths on the recorded spectra. An analogous analysis of a natural sugar sample results in a one factor PARAFAC solution, probably because of the large amount of different substances found in a table sugar sample resulting in rather featureless emission spectra not so susceptible to influence by the instrumental settings. Finally, it is demonstrated that two-way unfold PLS, PARAFAC and Tucker regression models are able to predict the excitation and emission slit widths from the recorded emission spectra. The root mean square errors of prediction (RMSEP) are about 0·5 nm ($R \approx 0{\cdot}990$) for the excitation slit and 0·3 nm ($R \approx 0{\cdot}999$) for the emission slit. © 1996 by John Wiley & Sons, Ltd.

KEY WORDS fluorescence spectroscopy; slit widths; PARAFAC; Tucker; three-way regression; alternating regression

INTRODUCTION

Fluorescence spectroscopy has for decades been a versatile analytical tool in the chemical laboratory, mostly owing to its extreme sensitivity and selectivity when considering the spectral shapes produced by analysis of single chemical component solutions.[1,2] During our work with the fluorescence technique for fast on-line/at-line analyses in the food industry[3,4] we have made several investigations of the instrumental aspects of fluorescence spectroscopy,[5,6] including the influence of different scan velocities, lamps and slit width adjustments on the obtained spectra. These investigations have primarily been concerned with the performance of the instrument when using the recorded spectra in a black box fashion with multivariate calibration models for e.g. the prediction of relevant quality parameters in sugar production. During these analyses we became attentive to the more general problem of how to understand the effect of different slit width adjustments on the

CCC 0886–9383/96/060615–16 $17.50

recorded spectra. In the analytical chemical literature, little has been published in this area (consult e.g. the reviews on fluorescence spectroscopy in *Analytical Chemistry*[7,8]). This may be because the explanations presented in textbooks on fluorescence spectroscopy and instrumental analysis seem satisfactory for the application spectroscopist:[1,9,10] 'Generally wider slit widths are used for quantitative analysis where accurate absorbance measurements are required; narrower slits are employed for qualitative work where spectral detail is important' (Reference 10, p. 510). This quotation describes qualitatively the effects of changing the slit widths, but one might ask what the quantitative effects of these changes are, a question that becomes even more relevant considering the increasing use of whole fluorescence spectra in combination with chemometrics.[3,5,6,11–14]

In this paper, two- and three-way resolution techniques are used in the analysis of the slit width problem. The problem of two-way resolution methods such as alternating regression[15] and evolving factor analysis[16] is that the found solutions are not necessarily unique. By imposing restrictions on the data it is possible in some cases to obtain unique solutions by two-way methods. These uniqueness problems can be solved when increasing the order of the data structure from two to three. The PARAFAC method is capable of giving unique three-way array resolutions and several applications have been reported.[17,18] The slit width problem is attacked by analysing fluorescence spectral data produced by real sample measurements with a Perkin Elmer spectrofluorometer. Instead of assuming e.g. triangular structures[19] of the influence of changing the slit widths and using this in a hard modelling fashion a complete soft modelling approach is chosen. A standard block sample and a natural sugar sample are analysed at different excitation and emission slit width combinations, yielding three-way arrays of fluorescence intensities to be analysed. Both two-way (alternating regression) and three-way (PARAFAC and Tucker) methods are employed. Furthermore, a comparison between classical unfold PLS, PARAFAC and Tucker regression models is given with respect to the prediction of slit widths from the measured emission spectra.

EXPERIMENTAL

Instrumentation and programmes

All experiments are performed on a Perkin-Elmer LS 50B spectrometer. The Perkin-Elmer LS50 FLDM Instrument programme (version 4.00) is used for instrument control. Spectral data are converted to ASCII files by a programme made in the OBEY language furnished by Perkin-Elmer (OBEY, version 3.50). An OBEY programme made by S. Huckins, Perkin-Elmer, is applied to obtain the raw unsmoothed fluorescence emission spectra during spectrum recording. Uncorrected fluorescence emission spectra sampled with 0·5 nm intervals at a maximum scan velocity of 1500 nm min^{-1} are recorded in all experiments. The sample holder was thermostatted to $22{\cdot}0 \pm 0{\cdot}1\,^{\circ}C$. Calculations are performed with Matlab for Windows version 4.2c.1 (MathWorks, Inc.) and Unscrambler version 5.5 (CAMO A/S). A toolbox made by Claus A. Andersson, Food Technology, The Royal Veterinary and Agricultural University[20] was used for the PARAFAC and Tucker decompositions. The alternating regression algorithm was programmed in the Matlab language.

Experiment 1

A standard block consisting of ovalene (standard block 2 in the Perkin-Elmer C 520-7440 set) is measured at excitation wavelength 351 nm. Emission spectra in the range 400–585 nm are recorded at all possible combinations of the excitation slit width (range 3–15 nm with 1 nm step) and the emission slit width (range 3–20 nm with 1 nm step), giving rise to a 234

$(=13 \times 18) \times 371$ matrix. In this data structure the two slit width orders are combined to yield a two-way array. By nature the recorded data actually constitute a three-way array with dimensions 13 (excitation slit widths) × 371 (emission wavelengths) × 18 (emission slit widths). When analysing the three-way data structure the emission wavelength direction is reduced by utilizing only every fourth data point. This yields a $13 \times 93 \times 18$ array where the emission wavelengths cover the range 400–584 nm with 2 nm steps.

Experiment 2

A stock solution of sugar is prepared by dissolving 75·0 g of table sugar in 500·0 ml of doubly deionized water. Emission spectra at excitation wavelength 340 nm are recorded in the range 372–600 nm at 63 different slit width combinations. The excitation slit width is varied with 2 nm steps from 3 to 15 nm (seven levels), while the emission slit width is varied with 2 nm steps in the range 3 to 19 nm (nine levels). Every excitation–emission matrix measurement is made on a freshly pipetted sugar sample taken directly from the stock solution, i.e. 63 samples have been analysed. The three-way data structure obtained has the dimensions $7 \times 114 \times 9$ (excitation slits × emission wavelengths × emission slits), where the emission data point range has been reduced by using every fourth data point.

THEORY

Scalars are represented by italic lowercase letters (x). Lowercase bold-face letters ($\mathbf{x}$) are vectors (one-way arrays), capital bold-face letters ($\mathbf{X}$) are matrices (two-way arrays) and underlined capital bold-face letters ($\underline{\mathbf{X}}$) designate three-way arrays. Elements of two-way and three-way arrays are represented as x_{ij} and x_{ijk}, where x can be the measured fluorescence intensity. The reader is referred to the literature for thorough descriptions of the employed methods.[15,17,18,21–26]

Alternating regression

Suppose we have a two-way array $\mathbf{X}$ in which each row is a fluorescence emission spectrum (J wavelengths) of a sample containing different amounts of F fluorophores. If the number of samples analysed is I, we want to resolve the measured mixture emission spectra into the pure F spectra and to obtain the concentration levels of the analytes in each sample. That is, the equation that is to be solved is $\mathbf{X} = \mathbf{C}\mathbf{S}^{\mathrm{T}}$, where $\mathbf{X}$ ($I \times J$) is the raw data matrix, $\mathbf{C}$ ($I \times F$) is a concentration matrix and $\mathbf{S}$ ($J \times F$) is a spectrum matrix. The alternating regression (AR) method works by the repetitive solution of two regression problems[15] and the basic assumption is that the data structure is bilinear. Firstly, an estimate of e.g. $\mathbf{S}$ is achieved (either by filling with random numbers or by using e.g. the first F principal components). From this estimate, $\mathbf{C}$ is calculated by the least squares solution $\mathbf{C} = \mathbf{X}\mathbf{S}(\mathbf{S}^{\mathrm{T}}\mathbf{S})^{-1}$, then an improved estimate of $\mathbf{S}$ is obtained by calculating $\mathbf{S} = \mathbf{X}^{\mathrm{T}}\mathbf{C}(\mathbf{C}^{\mathrm{T}}\mathbf{C})^{-1}$ and this iteration is performed a sufficient number of times determined by e.g. the size of the residuals when reconstructing $\mathbf{X}$ from $\mathbf{C}$ and $\mathbf{S}$. In each iteration cycle, negative elements are set to zero, i.e. the assumption is that both concentration and spectral profiles are larger than or equal to zero.

PARAFAC

The more complex three-way generalization of AR is PARAFAC, which is also based on

conditional linearity assumptions (trilinearity). The PARAFAC model can be written as[25]

$$x_{ijk} = \sum_{f=1}^{F} a_{if} b_{jf} c_{kf} + e_{ijk} \tag{1}$$

where x_{ijk} is an element in $\underline{\mathbf{X}}$ and for a given F the norm of $\underline{\mathbf{E}}$ (with elements e_{ijk}) is minimized; a_{if}, b_{jf} and c_{kf} are defined to be elements in the matrices **A**, **B** and **C** respectively. In the three-way data structure described in Experiment 1 $\underline{\mathbf{X}}$ ($I \times J \times K$) is a $13 \times 93 \times 19$ array and the dimensions of the PARAFAC solutions **A** ($I \times F$), **B** ($J \times F$) and **C** ($K \times F$) become $13 \times F$, $93 \times F$ and $19 \times F$ respectively. The main advantage of PARAFAC is that the obtained solutions are unique except with respect to scaling transformations and permutations of the columns of **A**, **B** and **C**.[25] The PARAFAC algorithm used in the calculations presented below is based on an alternating least squares approach.[20]

Tucker

The three-way generalization of principal component analysis is represented by the Tucker model.[25,26]

$$x_{ijk} = \sum_{f=1}^{F} \sum_{g=1}^{G} \sum_{h=1}^{H} a_{if} b_{jg} c_{kh} g_{fgh} + e_{ijk} \tag{2}$$

where x_{ijk} is an element in $\underline{\mathbf{X}}$ and for a given combination of F, G and H the norm of $\underline{\mathbf{E}}$ (with elements e_{ijk}) is minimized. The three-way array $\underline{\mathbf{G}}$ is the core array. Again we define a_{if}, b_{jf} and c_{kf} to be elements in the matrices **A**, **B** and **C** respectively.[25] PARAFAC is a special case of the Tucker model with $F = G = H$ and a three-way identity core matrix. The Tucker solutions (**A**, **B**, **C** and $\underline{\mathbf{G}}$) contain rotational ambiguities,[25] but through the core array all possible three-way interactions can be modelled, making the Tucker model more flexible than the PARAFAC model. The Tucker calculations presented in this paper are based on an alternating least squares approach without constraints on the matrices **A**, **B**, **C** and $\underline{\mathbf{G}}$.[20]

Regression models

Multivariate calibration of three-way data has been offered some attention during the last 5–10 years in chemometrics. Most models are based on the unfolding of the three-way array into a two-way matrix, making it possible to use the well-founded algorithms of two-way PLS1 or PLS2 regression,[27] but making it difficult to interpret e.g. loadings with a large number of variables. A trilinear PLS algorithm has been developed by Ståhle[28] and the theory of a general multilinear PLS method has been presented by Bro.[29] Below the two-way multivariate calibration approach is straightforwardly extended to three-way arrays based on the PARAFAC and Tucker decompositions.

Assume that we want to make a calibration model capable of predicting the excitation slit width **y**, ($I \times 1$) from the three-way data presented in Experiment 1. Firstly, the three-way data array $\underline{\mathbf{X}}$ is decomposed by the PARAFAC algorithm, resulting in the matrices **A** ($I \times F$), **B** ($J \times F$) and **C** ($K \times F$). It is then possible to solve the model

$$\mathbf{y} = \mathbf{Ar} \tag{3}$$

by ordinary multiple linear regression or e.g. a PLS1 approach; **r** is the vector containing the regression coefficients. Test set validation and cross-validation can be performed in the normal way to estimate the optimal number of factors. For a new unknown sample the **a**-loadings are calculated from the sample matrix (**X**), **B** and **C** and next the predicted y is calculated from

equation (3). **A** can of course be exchanged with **C** (or **B**) if e.g. the emission slits are to be calibrated for. The main advantage of the PARAFAC regression model compared with other models is that the matrices **A**, **B** and **C** are unique and directly interpretable. The method for a Tucker decomposed array is completely analogous, inserting the Tucker **A**, **B** or **C** into equation (3). The **a**-loadings of an unknown sample are calculated from the sample matrix (**X**), **B**, **C** and $\underline{\mathbf{G}}$ (and vice versa if **B** or **C** is to be used in the regression).

RESULTS AND DISCUSSION

Two-way methods (principal component analysis and alternating regression)

Experiment 1

In Figures 1A to 1D, selected examples of the measured emission spectra in Experiment 1 are given. Small emission slit widths give rise to spectral shapes with a fine structure trading a high signal-to-noise ratio for spectral resolution, while the opposite holds for large emission slit widths (compare Figures 1A and 1B). The spectral shapes obtained when using small and large excitation slits respectively are more alike (Figures 1C and 1D). The main difference rests in the signal-to-noise ratio, which is larger when using a large excitation slit. Furthermore, we see that the influence of the emission slit width adjustment on the recorded fluorescence intensity level is much larger compared with the influence of the excitation slit width (compare Figures 1A and 1B with Figures 1C and 1D). A principal component analysis (PCA) of the mean centered two-way data structure produces three significant components. The score and loading plots are shown in Figures 2A and 2B respectively. The explained variances by these components are 99·21%, 0·66% and 0·09% respectively. Using the loadings as input (**S**) to the alternating regression algorithm results in the estimated emission spectra and amount (or 'concentration') profiles depicted in Figure 3. From these plots it is possible to describe both qualitatively and quantitatively the effects of changing the slits. All emission spectra are composed of different amounts of the three hidden spectra, which may be designated as coarse structure, medium coarse/fine structure and fine structure (Figure 3A). The amount (Figure 3B) of the coarse structure spectrum shows the same behaviour at all excitation slits: it increases with an increase in the emission slit. The amount of the fine structure spectrum increases slightly with the excitation slit and has a maximum at an intermediate emission slit width. Finally, the amount of the medium coarse spectrum is proportional to the excitation slit as well as the emission slit.

Three-way methods (Tucker and PARAFAC)

Experiment 1

The above two-way resolution may be non-unique and it is difficult to distinguish the effects of the excitation and emission slits. By arranging the data in a three-way cube, it is possible to employ the PARAFAC and Tucker methods in order to resolve the data into the true underlying emission spectra and also to have an idea of the contribution from both the excitation and the emission slits. Consider the data structure in Experiment 1 as a three-way data structure with dimensions $13 \times 93 \times 18$ (corresponding to excitation slit × emission wavelengths × emission slits of $I \times J \times K$). Mean centering of the unfolded two-way array $IK \times J$ is performed prior to modelling, i.e. the emission spectra are mean centred. By unfolding the three-way array into the three possible two-way arrays followed by rank determination of these arrays, it is possible to find the number of

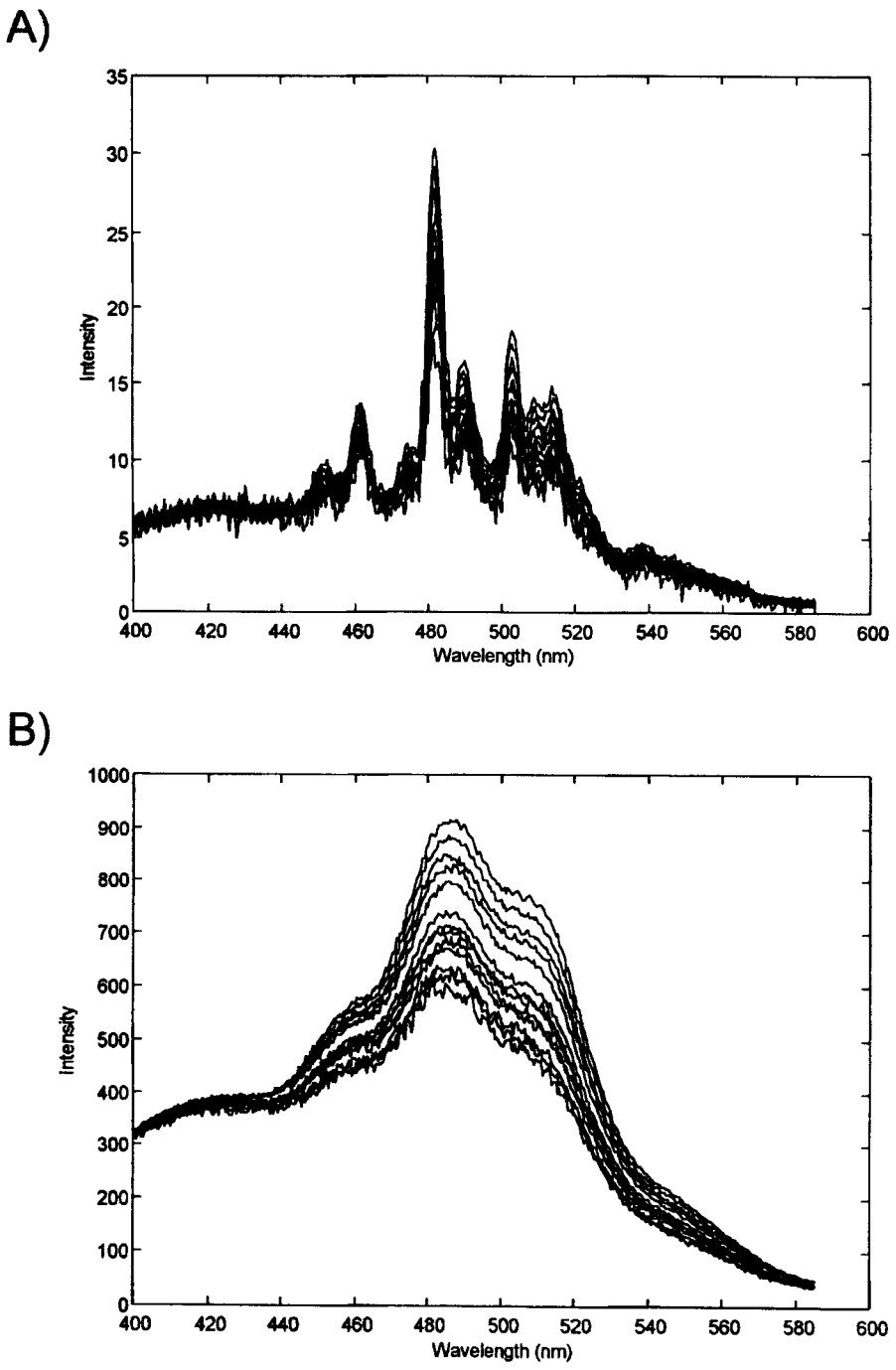

Figure 1. Fluorescence emission spectra (excitation 351 nm) from Experiment 1. (A) Thirteen spectra corresponding to excitation slits 3–15 nm and emission slit locked at 3 nm. (B) Same as A but with emission slit locked at 20 nm. (C) Eighteen spectra corresponding to emission slits 3–20 nm and excitation slit locked at 3 nm. (D) Same as C but with excitation slit locked at 20 nm

C)

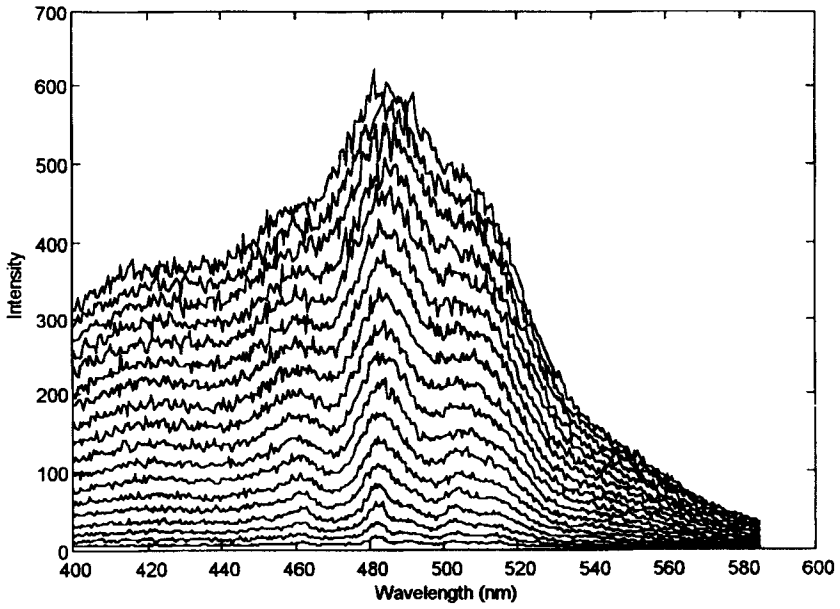

D)

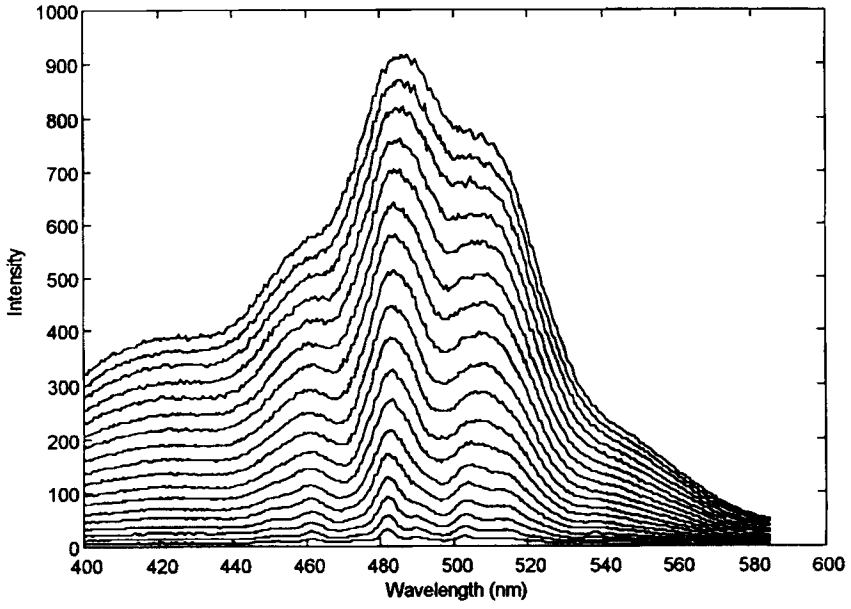

Figure 1. *Continued*

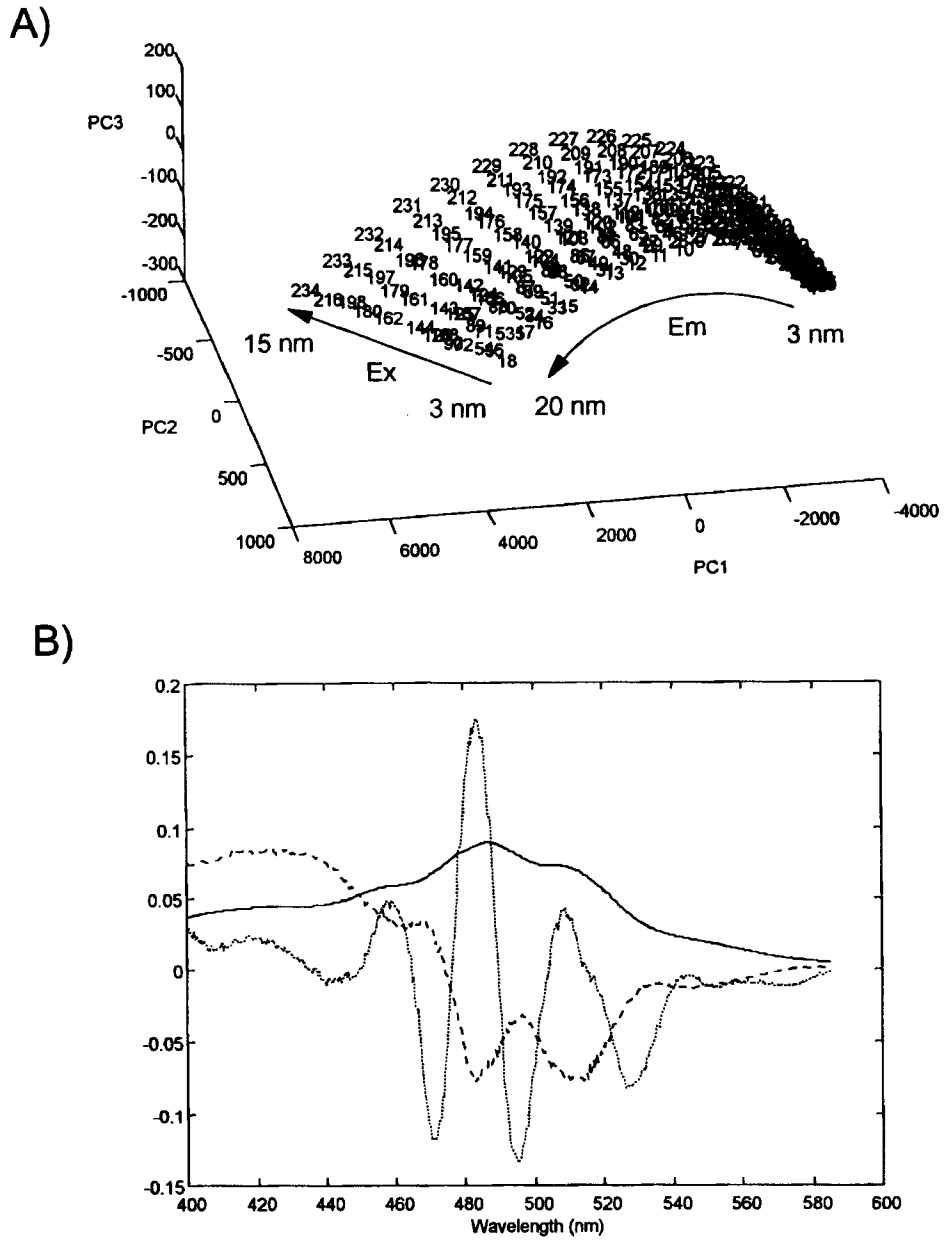

Figure 2. PCA on two-way data structure given in Experiment 1. (A) Score plot of first three score vectors. Numbers 1–18 correspond to emission slits 3–20 nm at excitation slit 3 nm, numbers 19–36 correspond to emission slits 3–20 nm at excitation slit 4 nm, etc. (B) Loading plot. Full curve, first loading; broken curves, second loading; dotted curve, third loading

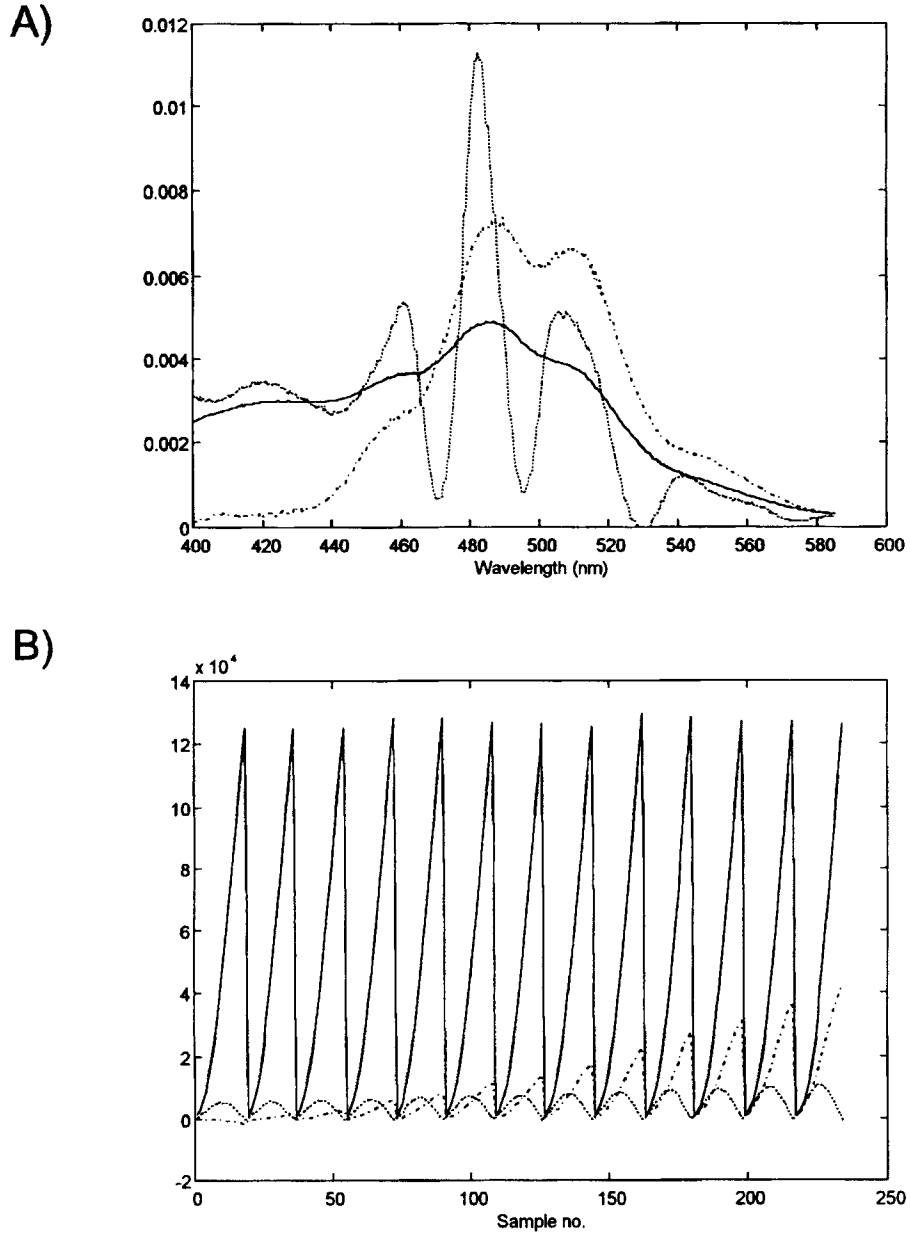

Figure 3. (A) Resolved spectra and (B) amount profiles by alternating regression of Experiment 1 two-way array. Line styles correspond in the plots. Sample numbering: see Figure 2. Full curve, first factor; broken curve, second factor; dotted curve, third factor

components to use in a Tucker model.[25] The ranks in the emission wavelength and emission slit directions are determined to be about three, while the rank in the excitation slit direction is about two. For a start a Tucker model with $F = G = H = 3$ was chosen. In Figure 4B the spectral loadings obtained by this analysis are shown. Comparing with Figure 2B, it is seen that the PCA loadings are almost identical with the smoother Tucker spectral loadings. In Figures 4A and 4C the

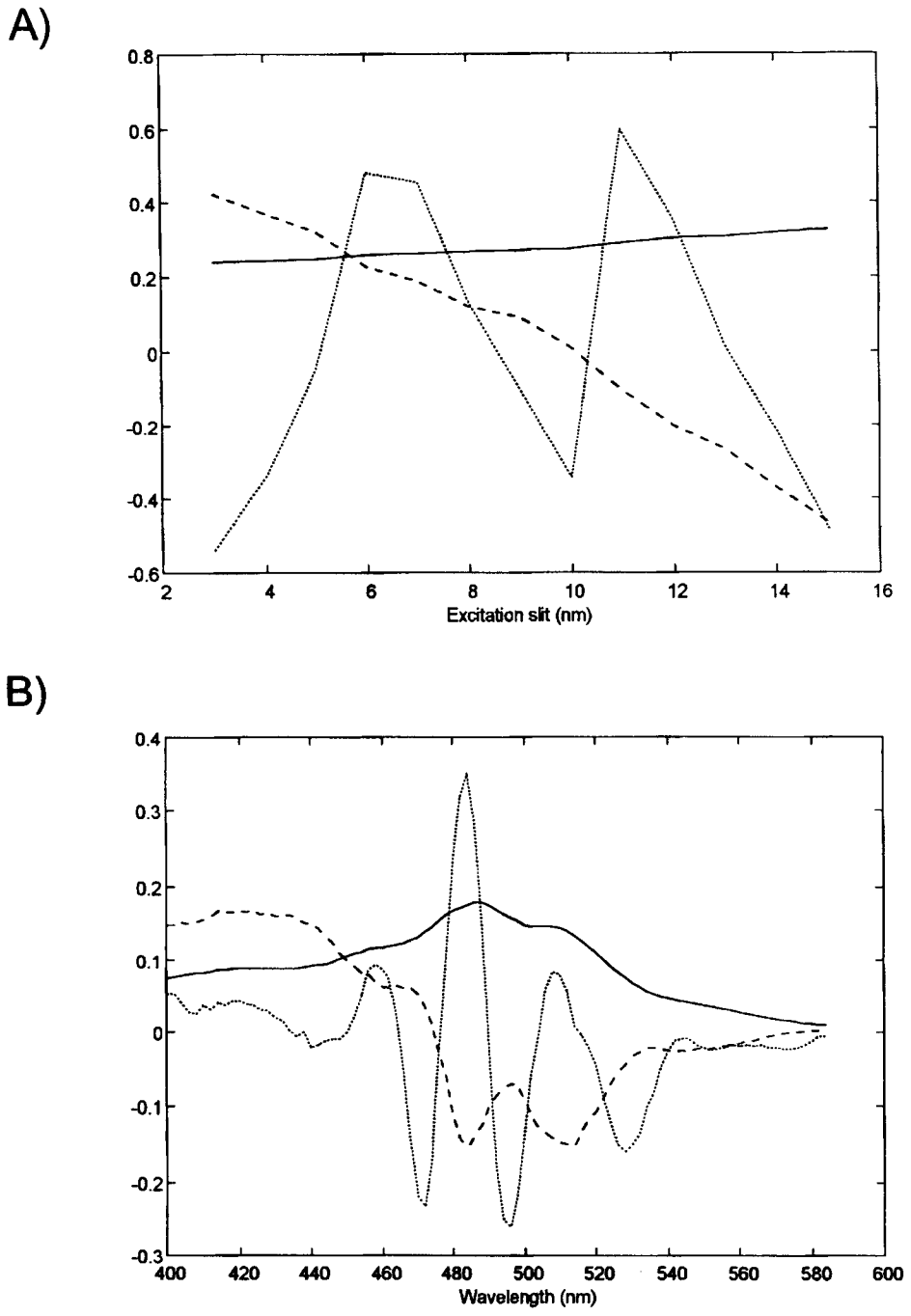

Figure 4. Tucker decomposition of the three-way data structure in Experiment 1. (A) Excitation slit loadings. (B) Spectral loadings. (C) Emission slit loadings. Line styles correspond in the plots. Full curve, first factor; broken curve, second factor; dotted curve, third factor

C)

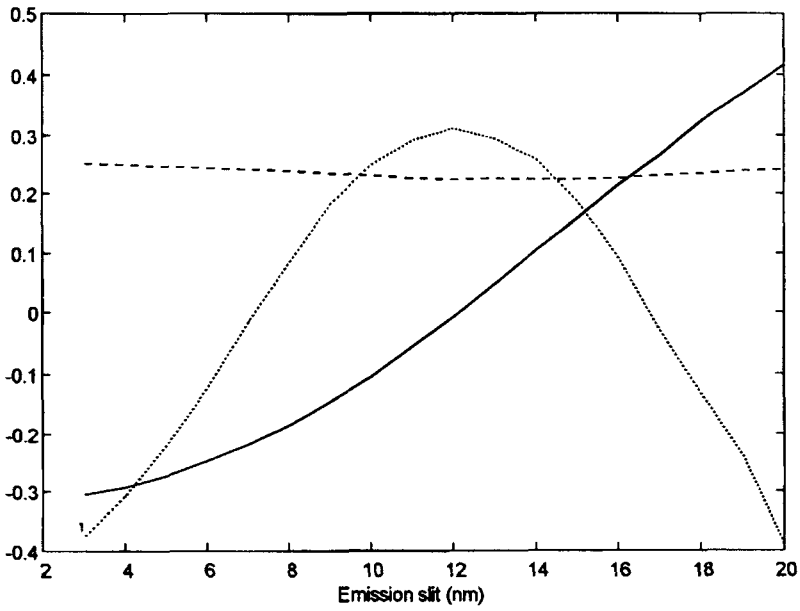

Figure 4. *Continued*

excitation and emission slit width loadings are given. It is now possible to analyse the separate contributions from the slits. The variance explained by the Tucker (3, 3, 3) model is 99·96%. Performing a Tucker (2, 3, 3) analysis gives almost identical loading matrices (except of course for the third excitation loading which is now missing), and the variance described by such a model is also 99·96%, indicating that only two dimensions are necessary in the excitation slit mode.

A PARAFAC analysis with three factors is also performed (also explaining 99·96% of the variance). Using four- or five-factor analysis, degenerate solutions are obtained (some loadings become almost identical). The solution matrices containing the slit width loadings have been normalized, resulting in the spectral loadings depicted in Figure 5B. Owing to the blow-up of the first spectral loading, both the second and third spectral loadings seem smoother than their Tucker counterparts (Figure 4B), but this is actually not the case when comparing the loadings on an equal scale. The PARAFAC excitation slit loadings (Figure 5A) are comparable with the corresponding Tucker loadings (Figure 4A), except for the third excitation loading which has become smooth in the PARAFAC solution. The third emission slit loadings have maxima at different slit widths, the Tucker loading seeming more in accordance with the third AR amount profile, while the second emission slit PARAFAC loading (Figure 5C) increases with increasing slit width as opposed to the second Tucker loading. The AR conclusions on the spectral structure (coarse, medium coarse/fine, fine) dependence of the slit width adjustments also hold for the Tucker and PARAFAC solutions (Figure 5B). Furthermore, the contributions from the different slits can now be interpreted directly from the score plots. In future research it will be interesting to investigate a PARAFAC method with non-negativity constraints on the loading matrices in order to achieve positive solutions (from the non-centred data) as well as restricted Tucker models also taking into account a lower rank of the excitation slit direction.

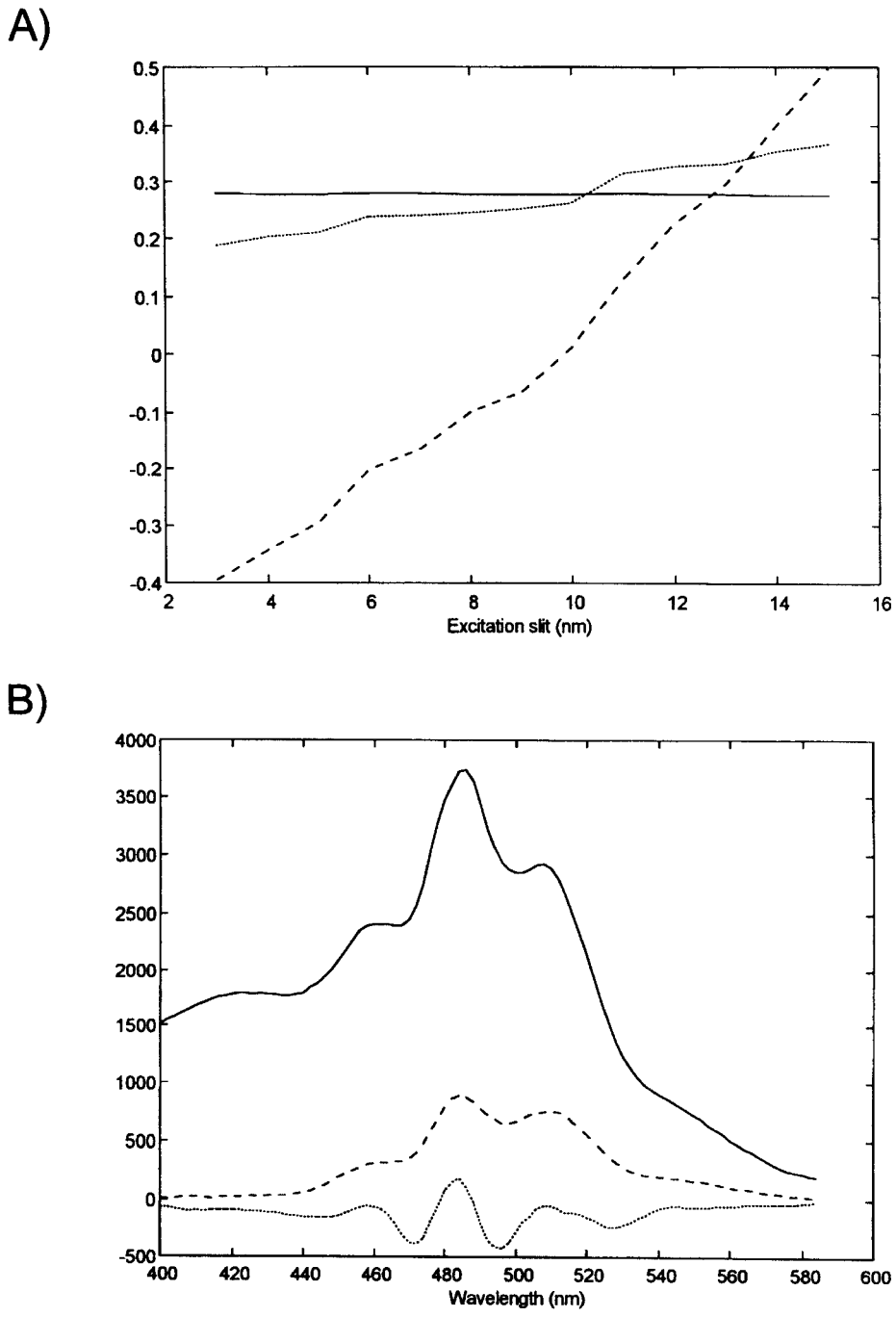

Figure 5. Three-factor PARAFAC decomposition of three-way data structure in Experiment 1. (A) Excitation slit loadings. (B) Spectral loadings. (C) Emission slit loadings. Line styles correspond in the plots. Full curve, first factor; broken curve, second factor; dotted curve, third factor

C)

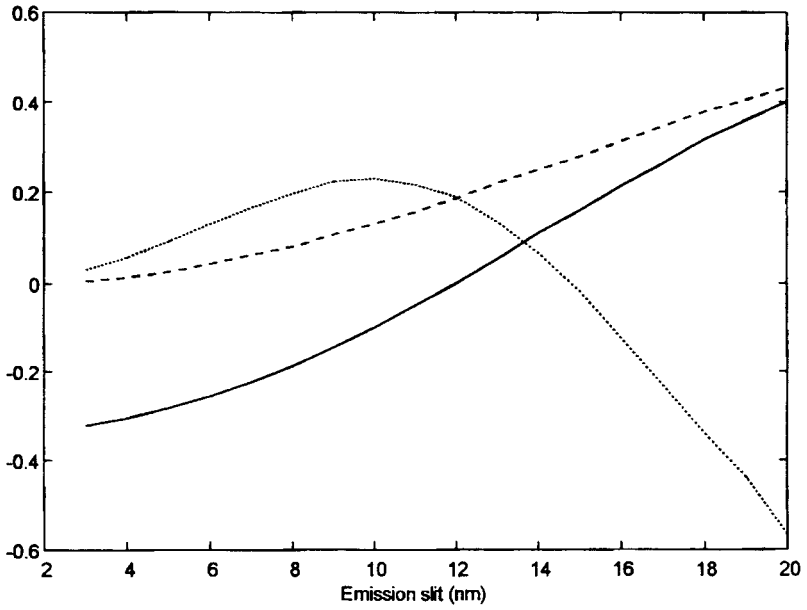

Figure 5. *Continued*

Experiment 2

It has previously been demonstrated that the behaviour of standard samples is different from the behaviour of natural samples when using fluorescence spectroscopy.[30] To investigate the slit width effect on natural samples, a sugar sample is analysed. The complex composition of the sugar beet in combination with the influence of the different sugar processing steps results in a final sugar product with low concentration levels of a large amount of impurities, some of which are fluorescing, e.g. phenols, melanins and amino acids.[31] A two-factor PARAFAC analysis of the three-way array from Experiment 2 yields the spectral loading vectors seen in Figure 6. The second spectral loading is noisy and highly correlated to the first spectral loading indicating that a one-factor solution is sufficient. Owing to the multiple chemical components present in the sugar sample, the spectral shape is very broad and without structure. Since a one-factor solution is sufficient, the only major effect of changing the slits is a change in the signal-to-noise level, i.e. one might as well open the slits fully in order to obtain the best signal-to-noise ratio. This is in agreement with earlier published results,[5] where the effect of different slit width combinations on the performance of PLS predictions of sugar samples was investigated.

Comments and perspectives regarding slit width resolution

By introducing more excitation wavelengths, it is possible to obtain four-way arrays, and by including the scan velocity as a variable, we have five-way arrays covering all the major instrument settings of a modern spectrofluorometer. The advantages, if any, of such data structures in fluorescence spectroscopy remain to be investigated by suitable *N*-way methods. As seen from Figure 1, there is a large difference in the absolute noise level of different slit

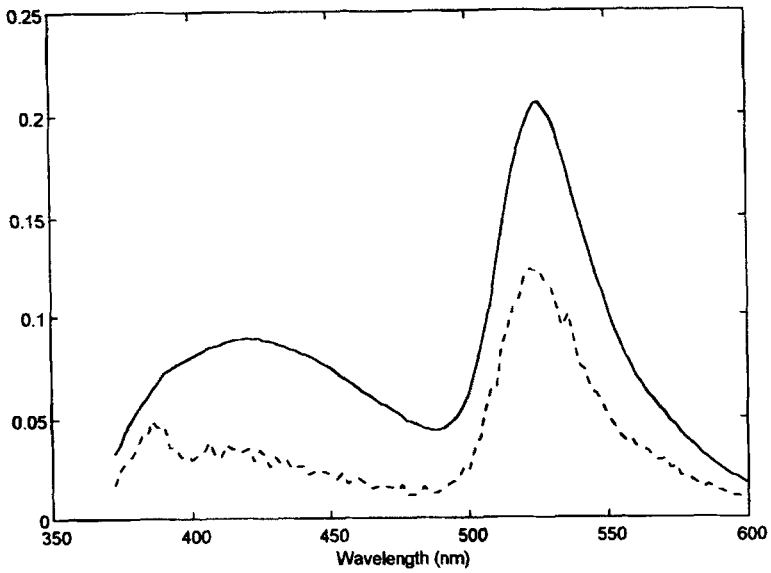

Figure 6. Spectral loadings from two factor PARAFAC decomposition of emission spectra measured on sugar sample (Experiment 2). Full curve, first factor; broken curve, second factor

combinations. This problem should be taken into account in future investigations knowing that the PARAFAC algorithm minimizes the residuals. Furthermore, a possible photodecomposition of the measured standard block should be considered in more detail in future experiments, even though the very good correlations (see below) between the measured spectra and the slit width adjustments imply that the variation seen is most likely due to slit width changes. One component solutions should be analysed in future experiments for comparison with the standard block spectra and spectrofluorometers of different makes should also be compared.

Regression models for the prediction of slit widths

It might be interesting in instrument calibration to be able to predict the slit width positions from a measured emission spectrum of a given standard. The two-way data structure presented in Experiment 1 (dimensions 234×371) is used as the independent matrix containing the spectral variables, while the excitation and emission slit widths are the variables to be predicted. In Table 1 the test set (117 samples, every second sample) prediction errors obtained by ordinary two-way PLS1 models are given. The linear PLS1 model is not capable of predicting the excitation slit widths, while the emission slit widths can be modelled. Utilizing the three-way data structure, it is possible to model also the excitation slit width as seen in Table 1, where the full cross-validated prediction results when using unfold PLS, PARAFAC MLR, and Tucker MLR on the three-way data structure from Experiment 1 are given. MLR means multiple linear regression, which is the method used in solving equation (3). If one wants orthogonal loadings as input to equation (3), the PARAFAC and Tucker decompositions can be made with orthogonal restrictions on the relevant loadings. It should be mentioned that in this preliminary study full cross-validation has been performed only in the regression step of the Tucker and PARAFAC models (equation (3)) and in the Tucker decomposition $F = G = H$. The emission slits are predicted with slightly smaller RMSEP values than the excitation slits. The performance differences between the calibration methods on the three-way data structure are very small, except from an interpretable point of view:

Table 1. Root mean square error of prediction (RMSEP) and correlation coefficient (R) for prediction of excitation and emission slit widths from emission spectra (see text). RMSEP = $[\sum_{i=1}^{N} (SW_i^{\text{predicted}} - SW_i^{\text{Reference}})^2/N]^{1/2}$, where $SW_i^{\text{Predicted}}$ is the model estimated slit width, $SW_i^{\text{Reference}}$ is the true slit width and N is the number of samples

		Number of samples	Number of factors	RMSEP	R
Two-way PLS[a]	Excitation	117	4	1·825	0·874
	Emission	117	3	0·367	0·998
Unfold PLS[b]	Excitation	13	2	0·544	0·990
	Emission	18	3	0·275	0·999
Tucker MLR[b]	Excitation	13	3	0·485	0·992
	Emission	18	3	0·337	0·998
PARAFAC MLR[b]	Excitation	13	4	0·487	0·992
	Emission	18	3	0·344	0·998

[a] Test set.
[b] Full cross-validation.

the loadings of the Tucker and PARAFAC models are much easier to inspect than the unfolded loadings of the PLS model (compare Figures 4AB and 5AB with Figure 7). Finally, a slight sigmoidal shape is seen in some of the predicted versus measured plots, indicating that a transformation of the dependent variable will lower the overall prediction errors further.

CONCLUSIONS

Two- and three-way resolution methods make it possible to quantify and interpret the spectral effects of changing the excitation and emission slit widths of a spectrofluorometer when analysing a standard block. By application of Tucker and PARAFAC methods it is possible to separate the effects of the slit adjustments of both monochromators. When analysing a sugar

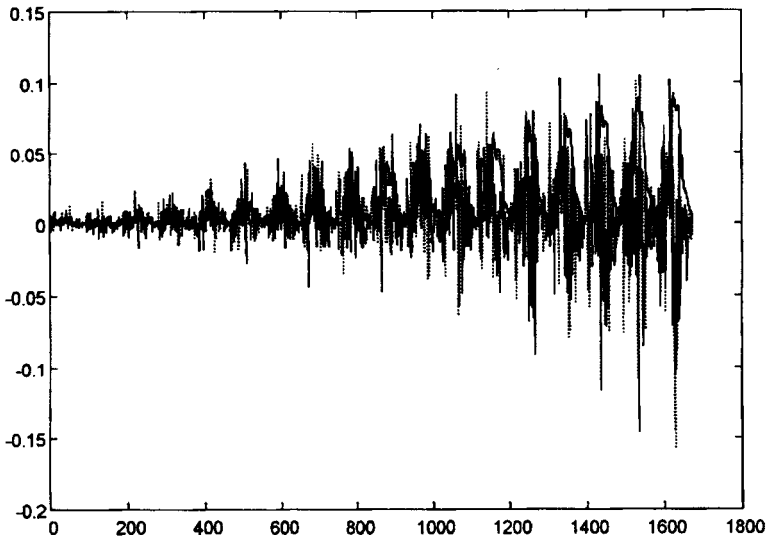

Figure 7. Unfold PLS loading weights when modelling excitation slit width. Full curve, first loading; dotted curve, second loading

sample in the same fashion, no significant spectral changes are observed, probably owing to the featureless broadband emission spectra originating from the fluorescence analysis of a sugar sample. This means that the slits might as well be fully open when analysing such samples. By means of unfold PLS, Tucker and PARAFAC regression both the excitation and emission slit widths can be predicted from a measured standard block emission spectrum.

ACKNOWLEDGEMENTS

Lars Munck is acknowledged for inspiring discussions during the preparation of the manuscript. Thanks are due to Rasmus Bro for valuable discussions and for introducing the *N*-way terminology at our laboratory. Thanks are also due to Claus A. Andersson for interesting discussions and for the programming of the Matlab three-way toolbox. The investigation is sponsored by funds to Professor Lars Munck from the Danish Research Councils 13-4804-1 (agriculture) and 16-5180-1 (technology) and from the Nordic Industry Foundation project P93149.

REFERENCES

1. G. Guilbault (ed.), *Practical Fluorescence*, 2nd edn, Marcel Dekker, New York (1990).
2. L. Munck (ed.), *Fluorescence Analysis in Foods*, Longman, London (1989).
3. L. Nørgaard, *Zuckerindustrie*, **120**, 970 (1995).
4. L. Nørgaard and R. Bro, C. A. Andersson, L. Munck, O. Hansen, L. B. Jørgensen and J. Jensen, *Proceedings for Conference on Sugar Processing Research*, New Orleans, USA (April 1996), in press.
5. L. Nørgaard, *Talanta*, **42**, 1305 (1995).
6. L. Nørgaard, *Chemometrics Intell. Lab. Syst.* **29**, 283 (1995).
7. S. A. Soper, L. B. McGown and I. M. Warner, *Anal. Chem.* **66**, 428R (1994).
8. I. M. Warner and L. B. McGown, *Anal. Chem.* **64**, 343R (1992).
9. C. A. Parker, *Photoluminescence of Solutions*, Elsevier, Amsterdam, 1968.
10. D. A. Skoog and D. M. West, *Fundamentals of Analytical Chemistry*, 4th edn, Holt-Saunders, Tokyo (1982).
11. S. A. Jensen, L. Munck and H. Martens, *Cereal Chem.* **59**, 477 (1982).
12. W. Lindberg, J.-Å. Persson and S. Wold, *Anal. Chem.* **55**, 643 (1983).
13. B. Pedersen and H. Martens, in *Fluorescence Analysis in Foods*, ed. by L. Munck, Chapt. 13, Longman, London (1989).
14. D. S. Burdick, X. M. Tu, L. B. McGown and D. W. Millican, *J. Chemometrics*, **4**, 15 (1990).
15. E. J. Karjalainen, *Chemometrics Intell. Lab. Syst.* **7**, 31 (1989).
16. M. Maeder and A. D. Zuberbühler, *Anal. Chim. Acta*, **181**, 287 (1986).
17. S. Leurgans and R. T. Ross, *Stat. Sci.* **7**, 289 (1992).
18. A. K. Smilde, *Chemometrics Intell. Lab. Syst.* **15**, 143 (1992).
19. Y. Senga, K. Minami, S. Kawata and S. Minami, *Appl. Opt.* **23**, 1601 (1984).
20. C. A. Andersson, *Three-way Toolbox*, http://newton.foodsci.kvl.dk/srccode.html (released 5 November 1995).
21. S. Wold, K. Esbensen and P. Geladi, *Chemometrics Intell. Lab. Syst.* **2**, 37 (1987).
22. H. Martens and T. Næs, Multivariate Calibration, 2nd edn, Wiley, New York 1993.
23. A. Höskuldsson, *J. Chemometrics*, **2**, 211 (1988).
24. E. Sanchez and B. R. Kowalski, *J. Chemometrics*, **4**, 29 (1990).
25. A. K. Smilde, Y. Wang and B. R. Kowalski, *J. Chemometrics*, **8**, 21 (1994).
26. R. Henrion, *Chemometrics Intell. Lab. Syst.* **25**, 1 (1994).
27. S. Wold, P. Geladi, K. Esbensen and J. Öhman, *J. Chemometrics*, **1**, 41 (1987).
28. L. Ståhle, *Chemometrics Intell. Lab. Syst.* **7**, 95 (1989).
29. R. Bro, *J. Chemometrics*, **10**, 47 (1996).
30. L. Munck, in *Fluorescence Analysis in Foods*, ed. by L. Munck, Chap. 1, Longman, London (1989).
31. R. F. Madsen, W. Kofod Nielsen, B. Winstrøm-Olsen and T. E. Nielsen, *Sugar Technol. Rev.* **6**, 49 (1978–1979).